EasyChair Preprint

№ 7863

Novel Elimination Method of Baseline Drift Based on Improved Least Square Method

Ruhao Zhang, Xin Xu, Yin Zhang and Tingting Xu

April 28, 2022

Novel Elimination Method of Baseline Drift Based on Improved Least Square Method

1st RuHao Zhang
School of Communication and Information Engineering
Nanjing University of Posts and Telecommunications
Nanjing, China
zrhujs@qq.com

2nd Xin Xu
School of Communication and Information Engineering
Nanjing University of Posts and Telecommunications
Nanjing, China
xuxin@njupt.edu.cn

4th Yin Zhang
School of Communication and Information Engineering
Nanjing University of Posts and Telecommunications
Nanjing, China
zyinzhang@163.com

3rd Tingting Xu
School of Communication and Information Engineering
Nanjing University of Posts and Telecommunications
Nanjing, China
ttx2010@gmail.com

***Abstract*—With the development of BCI, the application of bioelectrical signals have been widely used in various fields. Currently, the important issues is how to remove the interference from the signal. In the process of EMG signal acquisition, baseline drift is one of the most common disturbances. The LSM cannot remove the filtered baseline drift component within the window. To address this issue efficiently, a modified least method is designed in this paper, which remove the baseline drift component within the window by the curvature of the polynomial. The designed method can not only retain the advantages of the LSM small calculation volume, but also improve the baseline drift removal capability, providing a solution for embedded bioelectric signal acquisition device. Experimental results show that the ILSM has 5% improved to the conventional methods.**

***Index Terms*—baseline drift, electromyography, improved least square method, wavelet decomposition**

I. Introduction

It is Known that there exist many wheelchair users. However, most of the existing wheelchairs on the market use joystick control,which is big challenge, for patients with disabilities in their hands. To address this problem, some scholars have tried to use voice and blowing as the control means of wheelchairs. However, in practical usage, it has been found that these means are affected by the environment,e.g., the surrounding noise. Thus, more efficient methods need to be proposed urgently. Recently, the bioelectrical signal based on control methods have received a lot attention [1]. The authors in [2] used the muscle signals from arms to control wheelchair motion control. The wheelchair streering control is also achieved by observing the changes of brain waves under different flickering frequency light stimulation with the help of Electroencephalogram (EEG) signals [3]. Since both methods in [2] and [3], use electrical signals as a means of control, the signal-to-noise ratio of the collected bioelectrical signals has a great impact on the decision making of the controller. As the electrical signal is collected by the sensor, the body movement and the natural stretching of the skin can cause the changes of friction and pressure between the skin and the myoelectric acquisition sensor, which results in the fluctuations of the output signal from the sensor. This fluctuation can cause the output signal to jitter and drift up and down around the baseline. It was found by experiments that the baseline drift varies with the degree of friction between the skin, and the electromyographic(EMG) sensor is also affected by breathing, sweating, etc [4] . Since baseline drift causes up and down jitter in the electrical signal with random variations in amplitude and frequency, the usage of conventional high-pass filters is inefficient in addressing the baseline drift problem. In addition,the existence of baseline drift can also affect the various time and frequency domain indicators of EMG signal. Therefore, solving the baseline drift problem is one of the keys to improve the recognition accuracy of the system [5]. Currently, some schemes have been proposed the baseline drift problem in EMG signals. For example: 1) Adaptive trap filter scheme [4]. 2) Butterworth filter [6], [7]. 3) Ensemble empirical modal method [8], [9]. 4) Wavelet transform [10].5) Wavelet decomposition. 6) least square method (LSM) [11].

In the above scheme, LSM is very suitable for embedded medical devices because of its small computation and good effect. However, the traditional LSM cannot remove the baseline drift component within the window. To deal with this problem, this paper designs the improved least square method (ILSM), which polynomial and removes the baseline drift component from the EMG signal by the curvature of the polynomial. The experimental results show that ILSM can effectively remove the baseline drift component within the window. In addition, the computational complexity of the designed method is still low, which can guarantee that the designed method is suitable for the real-time applications.

We first introduce the relevant principles of the algorithm in Section II and demonstrate that ILSM has the advantage of small operation size by time complexity analysis. Experimental results are demonstrated in Section III. A comparative

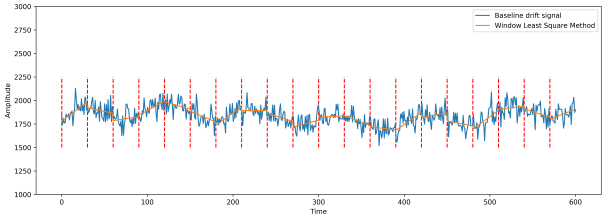

Fig. 1. The fitting function based on least square method.

analysis of the performance metrics of the algorithms is presented in Section IV. Finally, the conclusion and future work are given in Section V.

II. Principle and Proof of Algorithm

A. Principle of LSM

The traditional LSM is a computational tool widely used in error estimation, data prediction. It can be used to find trends in data and is often used for curve fitting.

EMG signal is a one-dimensional time series signal during the activity of the neuromuscular system. Through the electrical signal acquisition sensor, a set of electrical signals is recorded, which is denoted by x_i, where $i = 0, 1, \cdots, m-1$ is the sampling order.

To find a function that can match the trend of recorded data well, it is necessary compute the summation of distances from the function to each data point. It is noted that the best function is typically used, which can formulated as $P(x) = a+bx$ .The mean square error function can be obtained as:

$$Q(a,b) = \sum_{i=0}^{m-1} (p(x_i) - i)^2 = \sum_{i=0}^{m-1} (a + bx_i - i)^2 \quad (1)$$

If there is a point (a, b) that minimizes $Q(a, b)$, the function $P(x) = a+bx$ at the point (a, b) is the best-fit function of the EMG signal. Let a, b be the minimum point of $Q(a, b)$, then the partial derivative of $Q(a, b)$ with respect to point (a, b) is 0. After calculation, the fitting function can be obtained as shown in (2):

$$P(x) = \frac{\sum_{i=0}^{m-1} i \sum_{i=0}^{m-1} x_i^2 - \sum_{i=0}^{m-1} x_i \sum_{i=0}^{m-1} x_i i}{m\sum_{i=0}^{m-1} x_i^2 - (\sum_{i=0}^{m-1} x_i)^2} + \frac{m\sum_{i=0}^{m-1} x_i i - \sum_{i=0}^{m-1} x_i i \sum_{i=0}^{m-1} i}{m\sum_{i=0}^{m-1} x_i^2 - (\sum_{i=0}^{m-1} x_i)^2} x \quad (2)$$

Fig.1 depicts the fitting function based on LSM, where the red dashed line is the splitting line between the windows, the orange is the fitting function, and the blue is the original EMG signal. As can be seen from Figure 1, the orange line can show the trend of the EMG signal within the window, However, it cannot show the baseline drift trend of the EMG signal within the window. To address this problem, we can reduce the size of window to enhance the removal performance of baseline drift. However, this operation cannot totally remove the baseline drift component. According to [11] the window size is positively correlated with the performance of baseline drift removal. Decreasing the size of window is a way of removing the baseline drift component. However, as the window size increases, the computational complexity will increase exponentially.

B. Principle of the ILSM

In order to solve the problems of traditional LSM, we design the ILSM in this subsection. For the ILSM, a quadratic polynomial fitting is used to replace the linear segment fitting. Thus, the baseline drift component with the considered window can be removed by curvature of the quadratic function. By replacing the linear segment fitting used in the LSM with the polynomial $K_i(x) = a_i x^2 + b_i x + c_i$, and setting each segment to consist of $n(n < m)$ data, the ILSM equation can be obtained as follows:

$$P(x) = \begin{cases} a_1 x^2 + b_1 x + c_1, & x \in (1, N) \\ a_2 x^2 + b_2 x + c_2, & x \in (N, 2N) \\ \vdots & \\ a_N x^2 + b_N x + c_N, & x \in (m-N, m) \end{cases} \quad (3)$$

In (3), m is the total number of collected points of the electromyographic data, and n is the number of sampling points in each segment. The sum of the square of the distances between each point on $P(x)$ to each sampling point is called the cost function denoted as $Q(a, b, c)$, which is expressed as:

$$Q(a,b,c) = \sum_{i=0}^{m-1} (p(x_i) - i)^2 = \sum_{i=0}^{m-1} (ax_i^2 + bx_i + c - i)^2 \quad (4)$$

The best-fit curve is obtained when $Q(a, b, c)$ is minimum, each partial derivative is 0. Thus, setting the partial derivative of (4) with respect to a, b, c, to be zero, we have:

$$\begin{pmatrix} 2(\sum_{i=0}^{m-1} x_i^2)^2 & 2\sum_{i=0}^{m-1}(x^2+x) & 2\sum_{i=0}^{m-1} x_i^2 \\ 2\sum_{i=0}^{m-1}(x^2+x) & 2(\sum_{i=0}^{m-1} x)^2 & 2\sum_{i=0}^{m-1} x \\ 2\sum_{i=0}^{m-1} x^2 & 2\sum_{i=0}^{m-1} x & 2m \end{pmatrix} \begin{pmatrix} a \\ b \\ c \end{pmatrix} = \begin{pmatrix} 2\sum_{i=0}^{m-1} x^2 \sum_{i=0}^{m-1} i \\ 2\sum_{i=0}^{m-1} x^2 \sum_{i=0}^{m-1} i \\ 2\sum_{i=0}^{m-1} i \end{pmatrix} \quad (5)$$

As the determinant equation is not full-rank, more than one solution can be found for it. Thus, so the gradient descent algorithm can be used to find the optimal solution.

$$\begin{cases} a' = & a - W \times d_a \\ a' = & a - W \times d_a \\ a' = & a - W \times d_a \end{cases} \quad (6)$$

In (6), a', b', c' are the updated polynomial coefficients after calculation, and a, b, and c are the previous polynomial coefficients. W is the learning rate. d_a, d_b, d_c are the partial derivatives of a, b, and c. Using (6) to obtain updated polynomial coefficients a', b', c', we can then update the cost function, which is given by coefficients. Let the difference between the

cost function calculated from the new polynomial coefficients and the previous cost function be the gradient , denoted as $Q(a, b, c, a', b', c')$, which is giving by:

$$Y(a, b, c, a', b', c') = \sum_{i=0}^{m-1}(i - ax_i^2 - bx_i - c) - \sum_{i=0}^{m-1}(i - a'x_i^2 - b'x_i - c') \tag{7}$$

By computing (7), we can obtain the updated gradients of a, b, c. If the gradient is less than 0.01, the updated parameters a, b, c are considered to be the coefficients of the best-fit curve. Otherwise, the parameters a, b, c are not considered to be the optimal solutions at this time, and the above process is repeated until the optimal solution is found.

C. Comparative Analysis of the time complexity

Since wavelet decomposition and LSM are close to each other in terms of computation and denoising effect, and the time complexity of the ILSM is slightly increased, the time complexity of the two algorithms is compared to demonstrate the superiority of the ILSM. In order to explore the time consumed by the two algorithms in the same environment, this paper models the time complexity of the two algorithms in order to explore the time efficiency of the two algorithms. With N, I, A denoting the scale of the algorithm, the input of the algorithm, and the overall of the algorithm, respectively, and with T denoting the time complexity of the algorithm, there should be $T = (N, I, A)$. Since wavelet decomposition requires decomposing the signal into I layers, removing the low frequency part and then wavelet reconstruction to get the processed signal. According to the principle of wavelet decomposition algorithm, the time complexity model of wavelet decomposition algorithm can be constructed as:

$$T = 2n[1 - (\frac{1}{2})^I] \tag{8}$$

In (8), n is the number of sampling points, and I is the number of wavelet decomposition layers. where $2 \leq I \leq \log_2 n$.

Fig. 2 expresses the variation curve of time complexity with respect to the number of layers of wavelet decomposition I. Where, the time complexity of wavelet decomposition is a positive function with respect to I.

In the ILSM, the gradient descent algorithm is used to solve for the three coefficients of the second order polynomial. To solve the partial derivatives with respect to the coefficients it is also necessary to calculate the cumulative sum of each sampling point, which is used to solve the partial derivatives of each coefficient during each iteration.

In ILSM, in the process of solving the second-order polynomial coefficients with the help of gradient descent algorithm, it is necessary to iterate $\frac{n}{A}$ windows cyclically I times, and the time complexity of this step is denoted as $I * \frac{n}{A}$. It is also necessary to calculate the cumulative sum of each sampling point for use in the partial derivative calculation, and the time complexity of this step is n. Therefore, the time complexity model of ILSM can be obtained as:

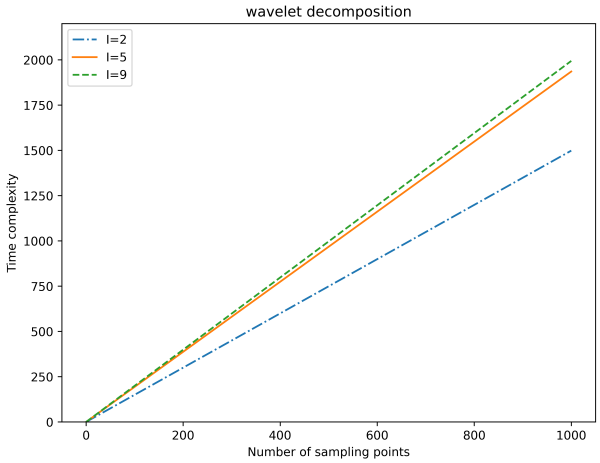

Fig. 2. Time complexity of wavelet decomposition algorithm under different I condition.

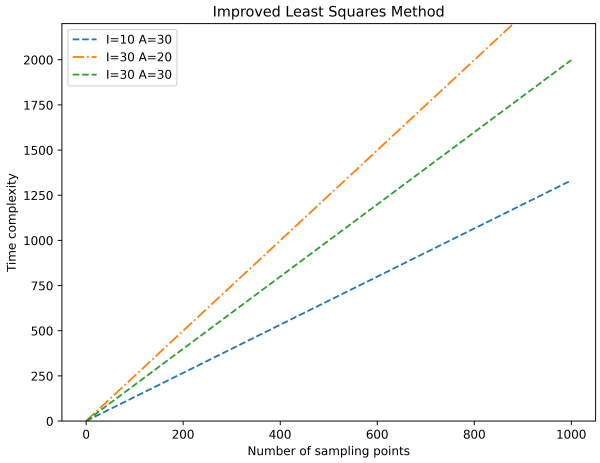

Fig. 3. Time complexity of improved least square method in different I cases.

$$T = n + I * \frac{n}{A} \tag{9}$$

where n is the number of sampling points, A is the window size, and $I(10 \leq I \leq 30)$ is the number of iterations.

Fig. 3 expresses the variation curve of time complexity with respect to the number of wavelet decomposition layers I and the window size A. Where, as can be seen from Fig. 3, the time complexity of ILSM is proportional to I and inversely proportional to A.

Fig. 4 depicts the comparative relationship between the time complexity of the ILSM and the wavelet decomposition method. As can be seen in Fig. 4, the time complexity of the ILSM is smaller than that of the wavelet decomposition algorithm when the window size is 30 and the number of iterations is 10.

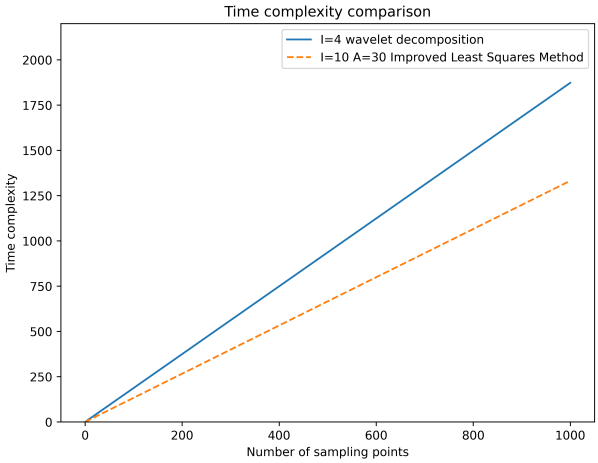

Fig. 4. Comparison of improved least square and wavelet decomposition algorithms.

TABLE I
COMPARISON OF DIFFERENT OBFUSCATIONS IN TERMS OF THEIR TRANSFORMATION CAPABILITIES

CPU	I7-9th
Operating Memory	32G
System	Win10
Simulation Software	VS code
Simulation Environment	Python3.0
High-pass filtering order	5
Low-pass filtering order	5
Wavelet decomposition	Db1

In summary, when the window size is larger than a certain value, the time complexity of the ILSM is much smaller than that of the wavelet decomposition method [12] [13].

III. EXPERIMENT AND PERFORMANCE ANALYSIS

In this chapter, the experimental data set used in the experiments is the humeral radial EMG signal acquired through the EMG single-lead muscle electrical sensor developed by Brain Lab. The hardware and software environment is shown in the following table.

To investigate the algorithm effectiveness, and reproducibility, experimental analysis is done in this section using own acquired sEMG signals of the brachioradialis muscle and sEMG signals from publicly available datasets, respectively [14] [15]. Since own acquisition of sEMG ensures a low baseline drift component, a baseline drift component can be added to investigate the ability of the algorithm to remove baseline drift and the effect on the useful signal. In the public dataset, since the signal itself already contains a more obvious baseline drift problem, it is not possible to add quantitative addition of baseline drift components to explore the metrics of the algorithm, only to demonstrate the effectiveness and generalizability of the algorithm.

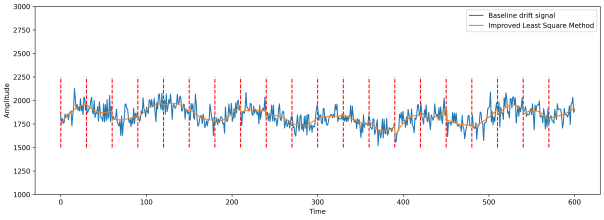

Fig. 5. Improved least square method fitting curve with a window size of 30 sampling points.

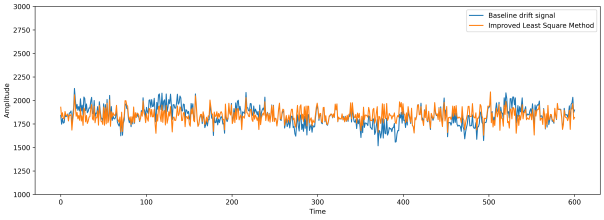

Fig. 6. Comparison pre and post improved least square method processing with a window size of 30 sampling points.

A. ILSM to remove baseline drift

Fig. 5 shows the fitted data trend function of ILSM with a window size of 30 . The blue line is the original EMG acquisition signal , the orange line is the fitted function for each segment of the EMG acquisition signal, and the red vertical segmentation line is the segmentation line for each segment. As can be seen from Fig. 5, the fitted function can accurately fit the trend function of the original EMG signal.

As shown in Fig. 6 and Fig. 7, Plots of amplitude versus time after ILSM processing are shown for window sizes of 10 and 30 sampling points, respectively. From the figures, it can be seen that the processing effect with a window size of 10 sampling points fits the baseline better than the one with a window size of 30 sampling points.

Fig. 8 and Fig. 9, respectively, show the relationship between magnitude and time after LSM processing under the window size of 10 and 30 sampling points. Comparing Fig. 6 and Fig. 7 with Fig. 8 and Fig. 9, we can see that the baseline drift still exists in the window of the function after using LSM processing, and changing the window size can optimize the problem, but it cannot remove the baseline drift from the root. After using ILSM, the baseline drift in the window is

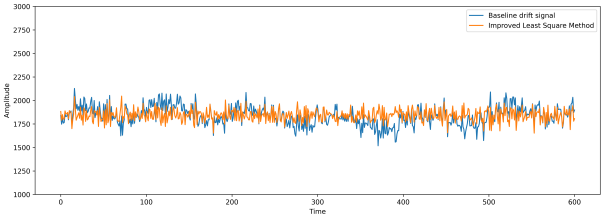

Fig. 7. Comparison pre and post improved least square method processing with a window size of 10 sampling points.

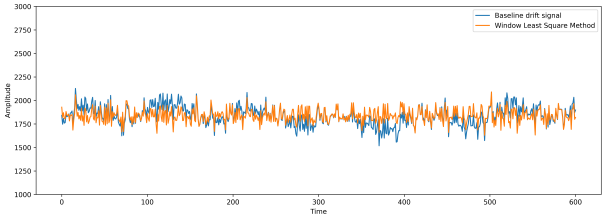

Fig. 8. Comparison of pre and post least square method processing with a window size of 30 sampling points.

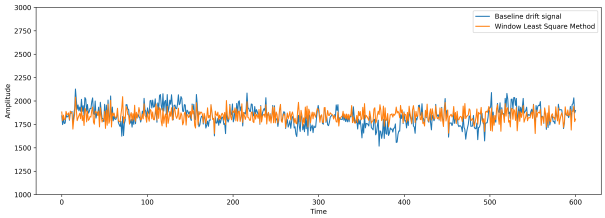

Fig. 9. Comparison of pre and post least square method processing with a window size of 10 sampling points.

effectively filtered out, so the filtering effect of ILSM is better than LSM with the same window size.

B. Performance Comparison of Higher Order LSM

In the previous subsection, the 2nd order polynomial ILSM is compared with the linear fit LSM, and the pictures in the time and frequency domains show that the 2nd order polynomial based LSM is better than the ILSM in terms of effectiveness. In this section, we investigate whether the LSM based on 3rd order polynomials outperforms the LSM based on 2nd order polynomials in terms of filtering effect and performance.

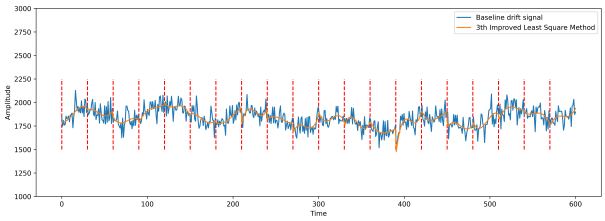

Fig. 10. 3rd order improved least square method curve fitting graph.

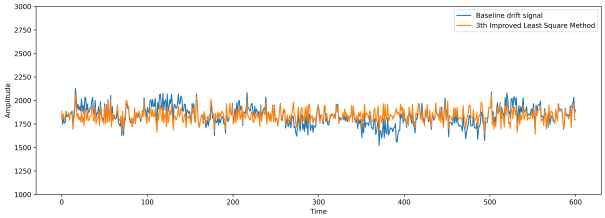

Fig. 11. Comparison of the 3rd order improved least square method with the original data.

TABLE II
COMPARISON OF THE TIMELINESS OF THE TWO ALGORITHMS

Order	Time (ms)
2rd order	4.05
3rd order	11.97

Fig.11 shows the effect of the 3rd order ILSM after processing. The orange line in the figure is the processed EMG signal waveform, and it can be seen that the baseline drift problem has been effectively improved.

In order to investigate the timeliness of the 2nd and 3rd order ILSM [16] [17], the time consumed by the two algorithms for processing data with the same window size is tested with a window size of 30 and 600 sampling points, as shown in Table II. As shown in Table II, the time required for the 3rd-order LSM is 2.95 times longer than that required for the 2nd-order LSM, which is not acceptable in embedded wearable devices because it consumes too much arithmetic power, so the performance of higher-order ILSM is not analysed and discussed in this paper.

IV. PERFORMANCE ANALYSIS

To measure the effectiveness of an algorithm, quantitative analysis of the signal is usually done in the time and frequency domains. In the time domain, a quantitative analysis of the algorithm's baseline drift removal metrics is done to observe the time domain metrics before and after the algorithm improvement. In the frequency domain, a spectral analysis of the EMG signal before and after the algorithm processing is done to observe two metrics whether the baseline drift component is effectively removed and whether the useful signal is attenuated. Since the EMG signals provided in the Ninapro database are unprocessed raw EMG signals, there is no guarantee that the EMG signals in the Ninapro database do not contain baseline drift components, so they are not suitable for quantitative analysis. Therefore, in this paper, an EMG single-conductor EMG sensor containing a hardware filter was used to acquire the signals and further filtered by a band-pass filter to ensure the purity of the raw signals. A sine wave superimposed at 2 Hz and 5 Hz with 1 signal-to-noise ratio is added to the original signal as the baseline drift content for quantitative analysis.

A. Time domain analysis

In the time domain, the degree of signal deviation from the baseline is mainly analysed. Therefore, Sample Mean Square Error (sMSE) can be used to observe the overall degree of variation of the signal and thus the ability of the algorithm to remove the baseline drift problem.

$$sMSE = \frac{\sum_{i=0}^{m-1}(x_i - \overline{x})^2}{m-1} \tag{10}$$

TABLE III
SAMPLE VARIANCE VALUES BEFORE AND AFTER ALGORITHM IMPROVEMENT

Signal	sMSE
Original signal	5819
Baseline drift signal	10375
LSM with a window size of 10	4381
ILSM with a window size of 10	4150
LSM with a window size of 30	5533
ILSM with a window size of 10	5331

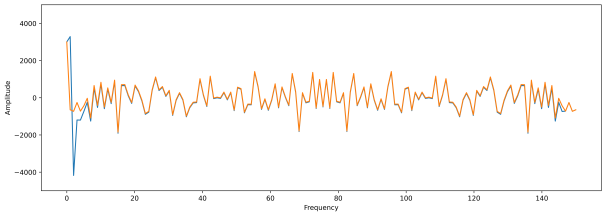

Fig. 12. Comparison of the spectrum of the original signal and the baseline drift signal.

where m is the number of sampling points, x_i is the i sampled EMG signal value, and $\bar{x}$ is the average of EMG signal sampling points.

As shown in Table III, the sMSE value of the EMG signal with the baseline drift added was 10375 and the sMSE of the original EMG signal was 5819, which shows that the EMG signal was significantly deviated after the baseline drift was added. With a window size of 10, the sMSE value of the LSM is 231 higher than that of the ILSM, and it can be seen that the ILSM is more effective in removing the baseline drift compared to before the improvement.

B. Frequency domain analysis

Fig.12 shows a comparison of the spectrum of the original signal and the signal with baseline drift, where the orange color is the spectrum of the original signal and the blue color is the spectrum of the signal with baseline drift. It can be observed that both the original signal and the signal with baseline drift have a high frequency density at 0 Hz, i.e., a high DC component is present. The signal with baseline drift has a high energy density at 1-5Hz, which corresponds to the frequency range where the baseline drift frequency is located.

Fig.13 and Fig.14 show the comparison of the original signal and the spectrum after processing by LSM for a window size of 30 and 10 sampling points, respectively. In the frequency domain of 10 Hz-150 Hz, comparing Fig.10 and Fig.15, it can be found that the original signal and the processed signal completely overlap in the frequency domain when the window size is 30 sampling points. In contrast, when the window size is 10 sampling points, there is a slight deviation in the frequency domain waveform after the LSM processing. This phenomenon indicates that LSM has a slight

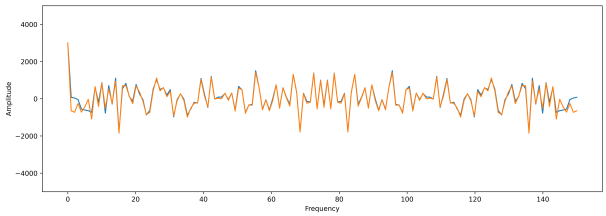

Fig. 13. Comparison of the original signal and the spectrum after least square method processing with a window size of 30 sampling points.

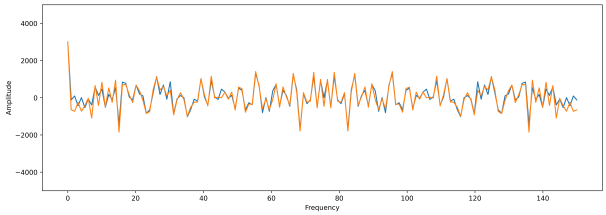

Fig. 14. Comparison of the original signal and the least square method processed spectrum with a window size of 10 sampling points.

effect on the useful signal portion at smaller windows. In the 0Hz-5Hz frequency domain band, comparing Fig.13 and Fig.14, it can be found that when the window size is 10 sampling points, the frequency domain content after LSM processing is smaller than the content after LSM processing with a window size of 30 sampling points. In summary, it can be concluded that by reducing the window size, the ability of the LSM algorithm to remove the baseline drift content can be improved. However, when the window is smaller than a certain value, it will have some effect on the useful signal segment.

Fig.15 depicts the comparison of the spectra of the original signal and the signal containing baseline drift after ILSM processing at a window size of 30 sampling points. In the 10Hz-150Hz frequency domain, comparing Fig.13 and Fig.15,

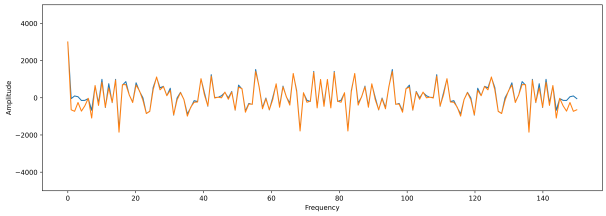

Fig. 15. Comparison of the original signal and the spectrum after improved least square method processing with a window size of 30 sampling points.

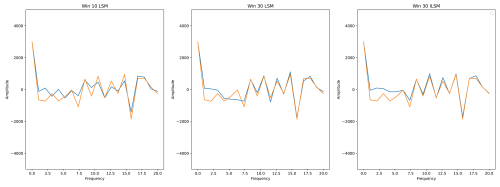

Fig. 16. Comparison of 0-20Hz waveforms in Figures 14, 15 and 16.

TABLE IV
SIGNAL REMOVAL RATE BEFORE AND AFTER ALGORITHM IMPROVEMENT

Signal	sRR(%)
With baseline drift signal	0
Original signal	100
Window size of 10 LSM	85.9
Window size of 10 ILSM	88.9
Window size of 30 LSM	79.0
Window size of 30 ILSM	81.9

it can be found that neither LSM nor ILSM has any effect on the useful signal components for the same window size. In the 0Hz-5Hz frequency domain, it can be found from Fig.16 that the baseline drift component in the ILSM-processed waveform is smaller than that in the LSM-processed waveform. In summary, ILSM has no significant effect on the useful signal compared to LSM with the appropriate window size, but ILSM has stronger attenuation effect on the baseline drift component in 0Hz-5Hz. Through Fig.12, Fig.13, Fig.14, and Fig.15, the advantages of ILSM over the LSM algorithm are perceptually observed from the spectrum, and the superiority of ILSM over LSM will be quantitatively analysed by mathematical equations in the following. In order to measure the ability of the two algorithms to remove baseline drift, a Signal Removal Rate (sRR) metric is used in this paper to measure the ability of the algorithm to remove baseline drift before and after the improvement of the algorithm, and its expression is:

$$sRR = 1 - \frac{\sum_{i=1}^{5} (|\widehat{p_i}| - |p_i|)}{\sum_{i=1}^{5} (|\ddot{p_i}| - |p_i|)} \tag{11}$$

Where, p_i is the i frequency power density of the original signal, $\sum_{i=1}^{2} |\widehat{p_i}|$ is the power density of 1 5Hz at which the baseline drift content is processed by the algorithm, p_i is the i frequency power density of the original signal, $\sum_{i=1}^{2} \ddot{p_i}$ is the power density of 1-5Hz at which the baseline drift of the signal with the baseline drift is added.

Table IV shows the signal removal rate of each algorithm under different window sizes. As can be seen from Table IV, under the same window, the improved algorithms are all improved by about 3% compared with the previous ones. In addition, it can be observed that the removal of baseline drift is better than before improvement under any window size. In order to measure whether the useful signal components are attenuated after the algorithm processing, this paper defines a Single Attenuation Rate (sAR) indicator to measure the attenuation of the useful signal, which is defined as:

$$sAR = 1 - \frac{\sum_{i=20}^{n} |\widehat{p_i}|}{\sum_{i=20}^{n} |p_i|} \tag{12}$$

Where n denotes the number of frequency analyses, p_i is the i frequency power density of the original signal, and $\widehat{p_i}$ is the i frequency power density after the algorithm removes the baseline drift problem.

TABLE V
SIGNAL ATTENUATION RATE PRE AND POST-ALGORITHM IMPROVEMENT

Signal	sAR(%)
Window size of 10 LSM	10.0
Window size of 10 ILSM	10.2
Window size of 30 LSM	1.8
Window size of 30 ILSM	2.1

Table V shows the signal attenuation rates of each algorithm for different window sizes. From Table V, it can be seen that the effects on the useful signals are similar pre and post-algorithm improvement with the same window size, and there is no big difference. However, it can be seen from Table V that although the smaller the window is, the better the baseline drift removal effect is, but it will cause some distortion of the signal and affect the useful signal content. In summary, from both the time domain and frequency domain, several indicators are summarized, based on the ILSM for the removal of baseline drift is about 3% more effective than the LSM, and the attenuation rate of the signal is similar to that before the improvement, so it can be seen that the algorithm is better than before the improvement in all aspects of the comprehensive indicators, with good baseline drift removal effect.

C. Comparative analysis of wavelet decomposition performance

In the previous subsection, it is verified that the performance index of ILSM is better than that of LSM in all aspects. since the wavelet decomposition algorithm is similar to LSM in terms of denoising effect, and the time complexity is close to that of LSM, this section will explore the performance comparison between ILSM and traditional wavelet decomposition algorithm. In this section, db1 wavelet is used to decompose the EMG signal, and after obtaining the wavelet coefficients of each layer, the low frequency content is removed and then the wavelet reconstruction is performed to analyze the parameters of the reconstructed EMG signal. According to the wavelet decomposition principle, the EMG sampling signal can be decomposed into 9 layers of wavelet coefficients, and the wavelet coefficients are removed in order from the first to the highest in the frequency domain, and the baseline drift problem is effectively filtered out when wavelet coefficients from 1 to 4 layers are retained.

As can be seen from Fig.17, the signal content at this time between 1 and 3 Hz is very close to the original signal.

As shown in Table VI, the performance indexes of wavelet coefficients of each layer are shown. From the data in the table, it can be found that the 3-layer wavelet coefficients have the best effect on the removal of baseline drift. Increasing or decreasing the number of wavelet layers will reduce the baseline drift removal effect. Therefore, it can be concluded

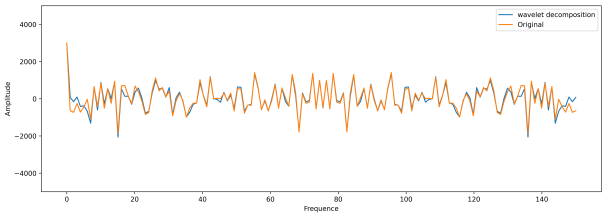

Fig. 17. Spectrum after reconstruction of 4-layer wavelet coefficients.

TABLE VI
PERFORMANCE INDEX OF WAVELET COEFFICIENTS OF EACH LAYER

layers	sMSE	sAR(%)	Time(ms)	sRR(%)
4	5403	4.2	6.18	80.4%
3	4919	8.0	4.98	83.0%
2	4094	10.6	2.95	79.3%

that the number of wavelet layers has a non-linear relationship with the removal effect of the baseline drift problem. In terms of processing time and loss rate, the higher the number of wavelet layers, the more time the algorithm takes, and conversely the lower the attenuation rate of the useful signal. In terms of mean square deviation, the lower the number of layers, the smaller the mean square deviation, indicating that the lower the number of layers the closer the signal is to the baseline and the less jitter, at the cost of reducing the useful signal content. Because of the large signal decay rate of the two-layer coefficients, the 3- and 4-layer wavelet coefficients are selected for performance comparison with LSM with different window sizes. As shown in Table VI.

As shown in Table VII, the 3-layer wavelet coefficients and the ILSM with a window size of 20 are close to each other in removing the baseline drift problem, but the wavelet decomposition algorithm takes less time. The sAR of both the 3-layer wavelet coefficients and the ILSM with a window size of 20 are large. sAR of both the 4-layer wavelet coefficients and the ILSM with a window size of 30 are smaller, and the sAR metric of the ILSM with a window size of 30 is half of that of the 4-layer wavelet coefficients. In terms of time, the ILSM is 2.13 ms faster than the four-layer wavelet coefficients, and the sRR metric is 1.5% higher.

TABLE VII
PERFORMANCE INDEXES OF ILSM AND WAVELET FRACTIONAL SOLUTION METHOD

Signal	sMSE	sAR(%)	Time(ms)	sRR(%)
Window size of 30 ILSM	5331	2.1	4.05	81.9
4 layers of small waves	5403	4.2	6.18	80.4
3 layers of small waves	4919	8.0	4.98	83.0
Window size of 20 ILSM	4816	7.7	7.97	83.9

V. CONCLUSION

In this article, we proposed ILSM to remove baseline drift, and some achievements are as follows: (1) This method improves the baseline drift removal rate. (2) The method can reduce the number of windows. (3)The ILSM used in this paper is close to the filtering effect of traditional wavelet transform and empirical modal methods in terms of performance, but the computation is much lower than traditional methods and the attenuation of useful signals is smaller. (4)And the method contributes to the less impact on the signal-to-noise ratio of the output signal.

REFERENCES

[1] Abayasiri RAM, Jayasekara AGBP, Gopura RARC et al. 2021 EMG Based Controller for a Wheelchair with Robotic Manipulator.
[2] Atrisandi AD, Adiprawita W, Mengko TLR et al. 2015 Noise and artifact reduction based on EEMD algorithm for ECG with muscle noises, electrode motions, and baseline drifts.
[3] Atzori M, Muller H. 2015 The Ninapro database: A resource for sEMG naturally controlled robotic hand prosthetics. Annu. Int. Conf. IEEE Eng. Med. Biol. Soc. IEEE Eng. Med. Biol. Soc. Annu. Int. Conf. pp.7151-7154.
[4] Boualem A, Meryem J, Ravier P et al. 2015 Legendre polynomial modeling of time-varying delay applied to surface EMG signals—Derivation of the appropriate time-dependent CRBs. Signal Process. pp.114.
[5] De Luca CJ, Gilmore LD, Kuznetsov M et al. 2010 Filtering the surface EMG signal: Movement artifact and baseline noise contamination. J. Biomech. pp.1573-1579.
[6] Hossain M-B, Bashar SK, Lazaro J et al. 2021 A robust ECG denoising technique using variable frequency complex demodulation. Comput. Methods Programs Biomed. 200: 105856.
[7] Huang C, Li W, Han S et al. 2018 A Novel Image Dehazing Algorithm Based on Dual-tree Complex Wavelet Transform. KSII Trans. Internet Inf. Syst. 12: 5039-5055.
[8] Luo Y, Hargraves RH, Belle A et al. 2013 A Hierarchical Method for Removal of Baseline Drift from Biomedical Signals: Application in ECG Analysis. Sci. World J. 2013: e896056.
[9] Nudra Bajantika Pradivta IW, Arifin A, Arrofiqi F et al. 2019 Design of Myoelectric Control Command of Electric Wheelchair as Personal Mobility for Disabled Person.
[10] Paul D, Mukherjee M. 2019 Automation of wheelchair using brain computer interface (BCI) technique. AIP Conf. Proc. 2072: 020004.
[11] Sbriccoli P, Bazzucchi I, Rosponi A et al. 2003 Amplitude and spectral characteristics of biceps Brachii sEMG depend upon speed of isometric force generation. J. Electromyogr. Kinesiol. Off. J. Int. Soc. Electrophysiol. Kinesiol. 13: 139-147.
[12] C. Ma et al., "Visual information processing for deep-sea visual monitoring system," vol. 1, pp. 3–11, Jan. 2021, doi: 10.1016/j.cogr.2020.12.002.
[13] H. Lu, Y. Zhang, Y. Li, C. Jiang, and H. Abbas, "User-Oriented Virtual Mobile Network Resource Management for Vehicle Communications," IEEE Transactions on Intelligent Transportation Systems, vol. 22, no. 6, pp. 3521–3532, Jun. 2021, doi: 10.1109/TITS.2020.2991766.
[14] Chinese image captioning via fuzzy attention-based DenseNet-BiLSTM, ACM Transactions on Multimedia Computing Communications and Applications, 2021.
[15] J. Sun and Y. Li, "Multi-feature fusion network for road scene semantic segmentation," Computers & Electrical Engineering, vol. 92, p. 107155, Jun. 2021, doi: 10.1016/j.compeleceng.2021.107155.
[16] Tyastuti FH, Aniroh Y, Muslimin D et al. 2017 Classification of EMG signal on arm muscle motion using special fourier transformation to control electric wheelchair.
[17] Zhang F, Tang X, Tong A et al. 2020 An Automatic Baseline Correction Method Based on the Penalized LSM. Sensors; 20: E2015